Study of anomalous $ZZ\gamma$ and $Z\gamma\gamma$ couplings at LEP

L3 Collaboration

M. Acciarri [ab], O. Adriani [q], M. Aguilar-Benitez [aa], S. Ahlen [l], J. Alcaraz [aa],
G. Alemanni [w], J. Allaby [r], A. Aloisio [ad], M.G. Alviggi [ad], G. Ambrosi [t],
H. Anderhub [aw], V.P. Andreev [g,al], T. Angelescu [n], F. Anselmo [j], A. Arefiev [ac],
T. Azemoon [c], T. Aziz [k], P. Bagnaia [ak], L. Baksay [ar], S. Banerjee [k], Sw. Banerjee [k],
K. Banicz [at], A. Barczyk [aw,au], R. Barillère [r], L. Barone [ak], P. Bartalini [w],
A. Baschirotto [ab], M. Basile [j], R. Battiston [ah], A. Bay [w], F. Becattini [q], U. Becker [p],
F. Behner [aw], J. Berdugo [aa], P. Berges [p], B. Bertucci [ah], B.L. Betev [aw],
S. Bhattacharya [k], M. Biasini [ah], A. Biland [aw], G.M. Bilei [ah], J.J. Blaising [d],
S.C. Blyth [ai], G.J. Bobbink [b], R. Bock [a], A. Böhm [a], L. Boldizsar [o], B. Borgia [r,ak],
D. Bourilkov [aw], M. Bourquin [t], S. Braccini [t], J.G. Branson [an], V. Brigljevic [aw],
I.C. Brock [ai], A. Buffini [q], A. Buijs [as], J.D. Burger [p], W.J. Burger [ah], J. Busenitz [ar],
A. Button [c], X.D. Cai [p], M. Campanelli [aw], M. Capell [p], G. Cara Romeo [j],
G. Carlino [ad], A.M. Cartacci [q], J. Casaus [aa], G. Castellini [q], F. Cavallari [ak],
N. Cavallo [ad], C. Cecchi [t], M. Cerrada [aa], F. Cesaroni [x], M. Chamizo [aa],
Y.H. Chang [ay], U.K. Chaturvedi [s], M. Chemarin [z], A. Chen [ay], G. Chen [h],
G.M. Chen [h], H.F. Chen [u], H.S. Chen [h], X. Chereau [d], G. Chiefari [ad], C.Y. Chien [e],
L. Cifarelli [am], F. Cindolo [j], C. Civinini [q], I. Clare [p], R. Clare [p], G. Coignet [d],
A.P. Colijn [b], N. Colino [aa], S. Costantini [i], F. Cotorobai [n], B. de la Cruz [aa],
A. Csilling [o], T.S. Dai [p], R. D'Alessandro [q], R. de Asmundis [ad], A. Degré [d],
K. Deiters [au], D. della Volpe [ad], P. Denes [aj], F. DeNotaristefani [ak], M. Diemoz [ak],
D. van Dierendonck [b], F. Di Lodovico [aw], C. Dionisi [r,ak], M. Dittmar [aw],
A. Dominguez [an], A. Doria [ad], M.T. Dova [s,1], D. Duchesneau [d], P. Duinker [b],
I. Duran [ao], S. Easo [ah], H. El Mamouni [z], A. Engler [ai], F.J. Eppling [p], F.C. Erné [b],
J.P. Ernenwein [z], P. Extermann [t], M. Fabre [au], R. Faccini [ak], M.A. Falagan [aa],
S. Falciano [ak], A. Favara [q], J. Fay [z], O. Fedin [al], M. Felcini [aw], T. Ferguson [ai],
F. Ferroni [ak], H. Fesefeldt [a], E. Fiandrini [ah], J.H. Field [t], F. Filthaut [r], P.H. Fisher [p],
I. Fisk [an], G. Forconi [p], L. Fredj [t], K. Freudenreich [aw], C. Furetta [ab],
Yu. Galaktionov [ac,p], S.N. Ganguli [k], P. Garcia-Abia [f], M. Gataullin [ag], S.S. Gau [m],

S. Gentile [ak], N. Gheordanescu [n], S. Giagu [ak], S. Goldfarb [w], J. Goldstein [l],
Z.F. Gong [u], A. Gougas [e], G. Gratta [ag], M.W. Gruenewald [i], R. van Gulik [b],
V.K. Gupta [aj], A. Gurtu [k], L.J. Gutay [at], D. Haas [f], B. Hartmann [a], A. Hasan [ae],
D. Hatzifotiadou [j], T. Hebbeker [i], A. Hervé [r], P. Hidas [o], J. Hirschfelder [ai],
W.C. van Hoek [af], H. Hofer [aw], H. Hoorani [ai], S.R. Hou [ay], G. Hu [e], I. Iashvili [av],
B.N. Jin [h], L.W. Jones [c], P. de Jong [r], I. Josa-Mutuberria [aa], R.A. Khan [s],
D. Kamrad [av], J.S. Kapustinsky [y], M. Kaur [s,2], M.N. Kienzle-Focacci [t], D. Kim [ak],
D.H. Kim [aq], J.K. Kim [aq], S.C. Kim [aq], W.W. Kinnison [y], A. Kirkby [ag], D. Kirkby [ag],
J. Kirkby [r], D. Kiss [o], W. Kittel [af], A. Klimentov [p,ac], A.C. König [af], A. Kopp [av],
I. Korolko [ac], V. Koutsenko [p,ac], R.W. Kraemer [ai], W. Krenz [a], A. Kunin [p,ac],
P. Lacentre [av,1,3], P. Ladron de Guevara [aa], I. Laktineh [z], G. Landi [q], C. Lapoint [p],
K. Lassila-Perini [aw], P. Laurikainen [v], A. Lavorato [am], M. Lebeau [r], A. Lebedev [p],
P. Lebrun [z], P. Lecomte [aw], P. Lecoq [r], P. Le Coultre [aw], H.J. Lee [i], J.M. Le Goff [r],
R. Leiste [av], E. Leonardi [ak], P. Levtchenko [al], C. Li [u], C.H. Lin [ay], W.T. Lin [ay],
F.L. Linde [b,r], L. Lista [ad], Z.A. Liu [h], W. Lohmann [av], E. Longo [ak], W. Lu [ag],
Y.S. Lu [h], K. Lübelsmeyer [a], C. Luci [r,ak], D. Luckey [p], L. Luminari [ak],
W. Lustermann [aw], W.G. Ma [u], M. Maity [k], G. Majumder [k], L. Malgeri [r],
A. Malinin [ac], C. Maña [aa], D. Mangeol [af], P. Marchesini [aw], G. Marian [ar,4], A. Marin [l],
J.P. Martin [z], F. Marzano [ak], G.G.G. Massaro [b], K. Mazumdar [k], R.R. McNeil [g],
S. Mele [r], L. Merola [ad], M. Meschini [q], W.J. Metzger [af], M. von der Mey [a],
D. Migani [j], A. Mihul [n], A.J.W. van Mil [af], H. Milcent [r], G. Mirabelli [ak], J. Mnich [r],
P. Molnar [i], B. Monteleoni [q], R. Moore [c], T. Moulik [k], R. Mount [ag], F. Muheim [t],
A.J.M. Muijs [b], S. Nahn [p], M. Napolitano [ad], F. Nessi-Tedaldi [aw], H. Newman [ag],
T. Niessen [a], A. Nippe [w], A. Nisati [ak], H. Nowak [av], Y.D. Oh [aq], G. Organtini [ak],
R. Ostonen [v], S. Palit [m], C. Palomares [aa], D. Pandoulas [a], S. Paoletti [ak,r],
P. Paolucci [ad], H.K. Park [ai], I.H. Park [aq], G. Pascale [ak], G. Passaleva [r], S. Patricelli [ad],
T. Paul [m], M. Pauluzzi [ah], C. Paus [r], F. Pauss [aw], D. Peach [r], Y.J. Pei [a], S. Pensotti [ab],
D. Perret-Gallix [d], B. Petersen [af], S. Petrak [i], A. Pevsner [e], D. Piccolo [ad], M. Pieri [q],
P.A. Piroué [aj], E. Pistolesi [ab], V. Plyaskin [ac], M. Pohl [aw], V. Pojidaev [ac,q],
H. Postema [p], J. Pothier [r], N. Produit [t], D. Prokofiev [al], J. Quartieri [am],
G. Rahal-Callot [aw], N. Raja [k], P.G. Rancoita [ab], M. Rattaggi [ab], G. Raven [an],
P. Razis [ae], D. Ren [aw], M. Rescigno [ak], S. Reucroft [m], T. van Rhee [as], S. Riemann [av],
K. Riles [c], A. Robohm [aw], J. Rodin [ar], B.P. Roe [c], L. Romero [aa], S. Rosier-Lees [d],
S. Roth [a], J.A. Rubio [r], D. Ruschmeier [i], H. Rykaczewski [aw], J. Salicio [r],
E. Sanchez [aa], M.P. Sanders [af], M.E. Sarakinos [v], C. Schäfer [a], V. Schegelsky [al],
S. Schmidt-Kaerst [a], D. Schmitz [a], N. Scholz [aw], H. Schopper [ax], D.J. Schotanus [af],
J. Schwenke [a], G. Schwering [a], C. Sciacca [ad], D. Sciarrino [t], L. Servoli [ah],
S. Shevchenko [ag], N. Shivarov [ap], V. Shoutko [ac], J. Shukla [y], E. Shumilov [ac],

A. Shvorob [ag], T. Siedenburg [a], D. Son [aq], B. Smith [p], P. Spillantini [q], M. Steuer [p], D.P. Stickland [aj], A. Stone [g], H. Stone [aj], B. Stoyanov [ap], A. Straessner [a], K. Sudhakar [k], G. Sultanov [s], L.Z. Sun [u], G.F. Susinno [t], H. Suter [aw], J.D. Swain [s], X.W. Tang [h], L. Tauscher [f], L. Taylor [m], C. Timmermans [af], Samuel C.C. Ting [p], S.M. Ting [p], S.C. Tonwar [k], J. Tóth [o], C. Tully [aj], K.L. Tung [h], Y. Uchida [p], J. Ulbricht [aw], E. Valente [ak], G. Vesztergombi [o], I. Vetlitsky [ac], G. Viertel [aw], M. Vivargent [d], S. Vlachos [f], H. Vogel [ai], H. Vogt [av], I. Vorobiev [r,ac], A.A. Vorobyov [al], A. Vorvolakos [ae], M. Wadhwa [f], W. Wallraff [a], J.C. Wang [p], X.L. Wang [u], Z.M. Wang [u], A. Weber [a], S.X. Wu [p], S. Wynhoff [a], J. Xu [l], Z.Z. Xu [u], B.Z. Yang [u], C.G. Yang [h], H.J. Yang [h], M. Yang [h], J.B. Ye [u], S.C. Yeh [az], J.M. You [ai], An. Zalite [al], Yu. Zalite [al], P. Zemp [aw], Y. Zeng [a], Z.P. Zhang [u], B. Zhou [l], G.Y. Zhu [h], R.Y. Zhu [ag], A. Zichichi [j,r,s], F. Ziegler [av], G. Zilizi [ar,4]

[a] *I. Physikalisches Institut, RWTH, D-52056 Aachen, FRG [5]*
III. Physikalisches Institut, RWTH, D-52056 Aachen, FRG [5]
[b] *National Institute for High Energy Physics, NIKHEF, and University of Amsterdam, NL-1009 DB Amsterdam, The Netherlands*
[c] *University of Michigan, Ann Arbor, MI 48109, USA*
[d] *Laboratoire d'Annecy-le-Vieux de Physique des Particules, LAPP,IN2P3-CNRS, BP 110, F-74941 Annecy-le-Vieux CEDEX, France*
[e] *Johns Hopkins University, Baltimore, MD 21218, USA*
[f] *Institute of Physics, University of Basel, CH-4056 Basel, Switzerland*
[g] *Louisiana State University, Baton Rouge, LA 70803, USA*
[h] *Institute of High Energy Physics, IHEP, 100039 Beijing, China [6]*
[i] *Humboldt University, D-10099 Berlin, FRG [5]*
[j] *University of Bologna and INFN-Sezione di Bologna, I-40126 Bologna, Italy*
[k] *Tata Institute of Fundamental Research, Bombay 400 005, India*
[l] *Boston University, Boston, MA 02215, USA*
[m] *Northeastern University, Boston, MA 02115, USA*
[n] *Institute of Atomic Physics and University of Bucharest, R-76900 Bucharest, Romania*
[o] *Central Research Institute for Physics of the Hungarian Academy of Sciences, H-1525 Budapest 114, Hungary [7]*
[p] *Massachusetts Institute of Technology, Cambridge, MA 02139, USA*
[q] *INFN Sezione di Firenze and University of Florence, I-50125 Florence, Italy*
[r] *European Laboratory for Particle Physics, CERN, CH-1211 Geneva 23, Switzerland*
[s] *World Laboratory, FBLJA Project, CH-1211 Geneva 23, Switzerland*
[t] *University of Geneva, CH-1211 Geneva 4, Switzerland*
[u] *Chinese University of Science and Technology, USTC, Hefei, Anhui 230 029, China [6]*
[v] *SEFT, Research Institute for High Energy Physics, P.O. Box 9, SF-00014 Helsinki, Finland*
[w] *University of Lausanne, CH-1015 Lausanne, Switzerland*
[x] *INFN-Sezione di Lecce and Universitá Degli Studi di Lecce, I-73100 Lecce, Italy*
[y] *Los Alamos National Laboratory, Los Alamos, NM 87544, USA*
[z] *Institut de Physique Nucléaire de Lyon, IN2P3-CNRS,Université Claude Bernard, F-69622 Villeurbanne, France*
[aa] *Centro de Investigaciones Energeticas, Medioambientales y Tecnologicas, CIEMAT, E-28040 Madrid, Spain [8]*
[ab] *INFN-Sezione di Milano, I-20133 Milan, Italy*
[ac] *Institute of Theoretical and Experimental Physics, ITEP, Moscow, Russia*
[ad] *INFN-Sezione di Napoli and University of Naples, I-80125 Naples, Italy*
[ae] *Department of Natural Sciences, University of Cyprus, Nicosia, Cyprus*
[af] *University of Nijmegen and NIKHEF, NL-6525 ED Nijmegen, The Netherlands*
[ag] *California Institute of Technology, Pasadena, CA 91125, USA*
[ah] *INFN-Sezione di Perugia and Universitá Degli Studi di Perugia, I-06100 Perugia, Italy*
[ai] *Carnegie Mellon University, Pittsburgh, PA 15213, USA*
[aj] *Princeton University, Princeton, NJ 08544, USA*
[ak] *INFN-Sezione di Roma and University of Rome, ''La Sapienza'', I-00185 Rome, Italy*
[al] *Nuclear Physics Institute, St. Petersburg, Russia*

am *University and INFN, Salerno, I-84100 Salerno, Italy*

an *University of California, San Diego, CA 92093, USA*

ao *Dept. de Fisica de Particulas Elementales, Univ. de Santiago, E-15706 Santiago de Compostela, Spain*

ap *Bulgarian Academy of Sciences, Central Lab. of Mechatronics and Instrumentation, BU-1113 Sofia, Bulgaria*

aq *Center for High Energy Physics, Adv. Inst. of Sciences and Technology, 305-701 Taejon, South Korea*

ar *University of Alabama, Tuscaloosa, AL 35486, USA*

as *Utrecht University and NIKHEF, NL-3584 CB Utrecht, The Netherlands*

at *Purdue University, West Lafayette, IN 47907, USA*

au *Paul Scherrer Institut, PSI, CH-5232 Villigen, Switzerland*

av *DESY-Institut für Hochenergiephysik, D-15738 Zeuthen, FRG*

aw *Eidgenössische Technische Hochschule, ETH Zürich, CH-8093 Zürich, Switzerland*

ax *University of Hamburg, D-22761 Hamburg, FRG*

ay *National Central University, Chung-Li, Taiwan, ROC*

az *Department of Physics, National Tsing Hua University, Taiwan, China*

Abstract

We search for anomalous $ZZ\gamma$ and $Z\gamma\gamma$ couplings with the L3 detector at LEP. The analysis is based on the study of the process $e^+e^+ \rightarrow Z\gamma$ at center-of-mass energies in the range $161\,\text{GeV} < \sqrt{s} < 183\,\text{GeV}$. No evidence for anomalous effects is found. Limits at the 95% confidence level are set on the values of the eight possible anomalous couplings. Depending on the type of coupling new physics scales below 213 GeV to 1083 GeV are excluded. © 1998 Elsevier Science B.V. All rights reserved.

1. Introduction

Deviations from the Standard Model expectation in the process $e^+e^+ \rightarrow Z\gamma$ are a clear sign of new physics [1,2]. Effects arising from $ZZ\gamma$ and $Z\gamma\gamma$ couplings are extremely small in the Standard Model [1,3], but can be enhanced in compositeness models [4,5] or if new particles enter in higher order corrections. The Standard Model cross section decreases rapidly as a function of the center-of-mass energy whereas anomalous contributions do not. The fact that the Z boson and the photon are produced far above threshold at current LEP energies is an additional advantage in sensitivity with respect to Z pole energies and with respect to other anomalous triple boson couplings [6]. Previous limits on $ZZ\gamma$ and $Z\gamma\gamma$ anomalous couplings have been published by the Tevatron [7–9] and LEP [10,11] experiments.

The $e^+e^+ \rightarrow Z\gamma$ Standard Model process at lowest order takes place through electron-exchange in the *t*-channel. For a collision in the center-of-mass reference frame the photon is emitted with an energy $E_\gamma = \frac{\sqrt{s}}{2}(1 - \frac{m_Z^2}{s})$, where $\sqrt{s}$ is the energy of the collision. The main experimental signature of the $e^+e^+ \rightarrow Z\gamma$ process is thus the production of an almost monoenergetic photon of very high energy.

Anomalous $ZZ\gamma$ and $Z\gamma\gamma$ couplings would manifest themselves as a global enhancement of the number of $Z\gamma$ events, especially when the photon is emitted at large angles with respect to the beam axis. Another anomalous effect is an excess in the number of longitudinally polarized Z bosons, which influences the angular distributions of the fermions. CP-

violating couplings may produce asymmetric angular distributions. In particular, an asymmetric polar angle distribution of the photon would be a direct signal of CP violation [12,13].

In the following analysis the most sensitive channels, $e^+e^- \to q\bar{q}\gamma(\gamma)$ and $e^+e^- \to \nu\bar{\nu}\gamma(\gamma)$, are used to set limits on anomalous $ZZ\gamma$ and $Z\gamma\gamma$ couplings. The data sample collected with the L3 detector [14] comprises an integrated luminosity of 74 pb at center-of-mass energies between 161 GeV and 183 GeV.

2. Event selection

The selection of $Z\gamma$ events requires the presence of an energetic photon in the event. This photon is identified as a cluster in the BGO calorimeter with more than 90% of its energy deposited in a 3×3 crystal matrix and satisfying $80 \text{ GeV} < (s - 2E_\gamma\sqrt{s})^{1/2} < 110 \text{ GeV}$.

This requirement ensures a recoil against a system of invariant mass consistent with a Z. It implies photon energies between 43 GeV and 74 GeV for the center-of-mass energy range covered by this analysis. Specific cuts for $q\bar{q}\gamma$ and $\nu\bar{\nu}\gamma$ events are presented in the following subsections.

In the estimation of signal and background processes the following Monte Carlo generators have been used: PYTHIA [15] for $e^+e^- \to q\bar{q}(\gamma)$, $e^+e^- \to Z/\gamma^* \gamma \to q\bar{q}\gamma$, KORALZ [16] for $e^+e^- \to \nu\bar{\nu}\gamma(\gamma)$, EXCALIBUR [17] for $e^+e^- \to q\bar{q}\ell\nu$, $e^+e^- \to e\nu_e\ell\nu_\ell$, PHOJET [18] for $e^+e^- \to e^+e^-$ hadrons and BHAGENE [19], TEEGG [20] for $e^+e^- \to e^+e^-\gamma(\gamma)$. All generated events are passed through
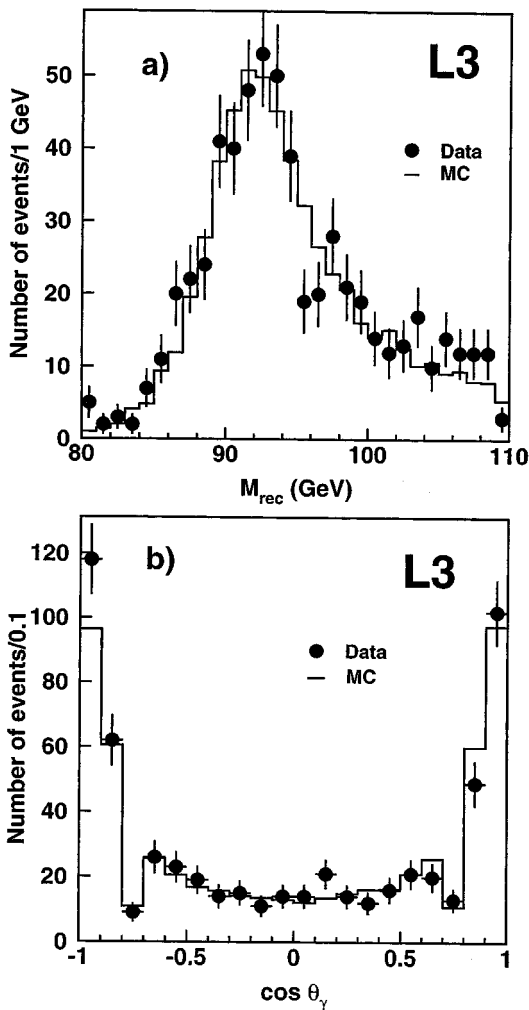

Fig. 1. Distributions of a) the mass recoiling against the photon $M_{rec} = (s - 2E_\gamma\sqrt{s})^{1/2}$ and b) the polar angle of the photon in $e^+e^- \to q\bar{q}\gamma(\gamma)$ events. Dots are data and the histograms are the Standard Model Monte Carlo prediction.

a simulation of the L3 detector response [21] and through the same analysis program used for the data. The detector response as a function of time is taken into account.

2.1. Selection of $e^+e^- \to q\bar{q}\gamma(\gamma)$ events

In addition to the presence of a photon recoiling to the Z, high multiplicity and energy-momentum balance are required to select $e^+e^- \to q\bar{q}\gamma(\gamma)$ events:

- The polar angle of the photon must satisfy $14° < \theta_\gamma < 166°$.

Table 1
Measured cross sections σ of the process $e^+e^- \to q\bar{q}\gamma(\gamma)$ at center-of-mass energies in the range 161 GeV to 183 GeV. $\mathcal{L}$ indicates the integrated luminosity. Quoted cross sections and acceptances ϵ correspond to generated events with one radiated photon with energy greater than 20 GeV and a polar angle in the range $5° < \theta_\gamma < 175°$. The Standard Model cross sections [15] σ_{SM} are listed in the rightmost column.

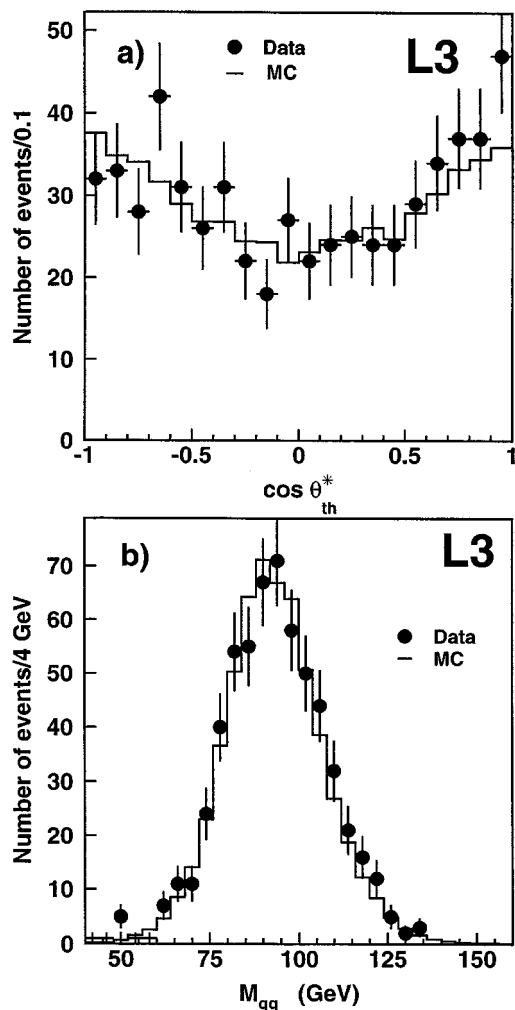| $\sqrt{s}$ (GeV)	$\mathcal{L}$ (pb)	ϵ (%)	Events	σ (pb)	σ_{SM} (pb)
161	9.95	37.0 ± 0.6	117	30.2 ± 3.0	27.6
170	0.97	33.4 ± 0.5	7	20.4 ± 7.1	25.0
172	8.48	35.1 ± 0.6	59	18.7 ± 2.3	23.3
183	55.30	30.9 ± 0.2	410	22.3 ± 1.2	21.6

Fig. 2. Distributions of a) the polar angle distribution of the hadronic thrust axis θ_{th}^* and b) the measured invariant mass $M_{q\bar{q}}$ in $e^+e^+ \to q\bar{q}\gamma(\gamma)$ events. The thrust angle is measured in the rest frame of the $q\bar{q}$ system, defined by a boost along the photon direction with velocity $v_Z = E_\gamma /(\sqrt{s} - E_\gamma)$.

- The number of tracks in the event must be greater than 6 and the number of calorimetric clusters must exceed 11.
- The transverse and longitudinal energy imbalances in the event must be less than 15% and 20% of the visible energy, respectively.

With these criteria 593 events are selected in the center-of-mass energy range from 161 GeV to 183 GeV. The acceptance of these cuts is estimated with the PYTHIA Standard Model $e^+e^+ \to Z/\gamma^* \gamma \to$

$q\bar{q}\gamma$ generator [15]. Due to the redundancy of multiplicity and energy triggers, the trigger inefficiency is estimated to be negligible.

Two backgrounds were found to have a non-negligible contribution: a) $e^+e^+ \to q\bar{q}\,e\,\nu$, where the electron fakes a photon, giving a 1.5% contamination in the data sample and b) $e^+e^+ \to q\bar{q}(\gamma)$ events, mainly due to misidentified π^0 which contribute 0.5%. Using the measured luminosities, the number of selected events and the estimated acceptance we obtain the cross sections shown in Table 1. The quoted cross sections and acceptances correspond to generated events with at least one radiated photon with energy greater than 20 GeV and its polar angle in the range $5° < \theta_\gamma < 175°$. The measured cross sections are in agreement with the expectations from the Standard Model.

Fig. 1a and 1b show the recoiling mass distribution and the polar angle of the photons, respectively. The distribution of the thrust polar angle of the $q\bar{q}$ system in its rest frame is shown in Fig. 2a. The distribution of the $q\bar{q}$ invariant mass, shown in Fig. 2b, is consistent with the value of the Z mass and with the calorimetric resolution of the L3 detector. Good agreement between data and Standard Model is observed.

2.2. Selection of $e^+e^+ \to \nu\bar{\nu}\gamma(\gamma)$ events

In addition to the presence of a photon the selection criteria for the $e^+e^+ \to \nu\bar{\nu}\gamma(\gamma)$ channel take into account low multiplicity, large energy imbal-

Table 2
Measured cross sections σ of the process $e^+e^+ \to \nu\bar{\nu}\gamma(\gamma)$ at center-of-mass energies in the range 161 GeV to 183 GeV. $\mathscr{L}$ indicates the integrated luminosity. Quoted cross sections and acceptances ϵ correspond to generated events with one radiated photon with energy greater than 20 GeV and its polar angle in the range $5° < \theta_\gamma < 175°$. The Standard Model cross sections [16] σ_{SM} are listed in the rightmost column.

$\sqrt{s}$ (GeV)	$\mathscr{L}$ (pb)	ϵ (%)	Events	σ (pb)	σ_{SM} (pb)
161	10.32	28.5 ± 0.7	31	10.5 ± 2.2	8.2
170	0.99	28.2 ± 0.7	1	3.6 ± 2.6	7.0
172	8.79	28.7 ± 0.7	22	8.7 ± 2.1	6.9
183	52.55	31.9 ± 0.4	99	5.9 ± 0.6	5.5

ance, rejection of cosmic rays and the absence of charged tracks in the event:

- The polar angle of the photon must satisfy $16° < \theta_\gamma < 164°$.
- The number of reconstructed tracks in the event must be zero and the number of calorimetric clusters cannot exceed 10. The number of hits collected in the tracking chamber associated to a calorimetric cluster must not exceed 40% of the expected number of hits for a charged track.
- The transverse and total energy imbalances in the event must be greater than 20% and 95% of the visible energy, respectively.
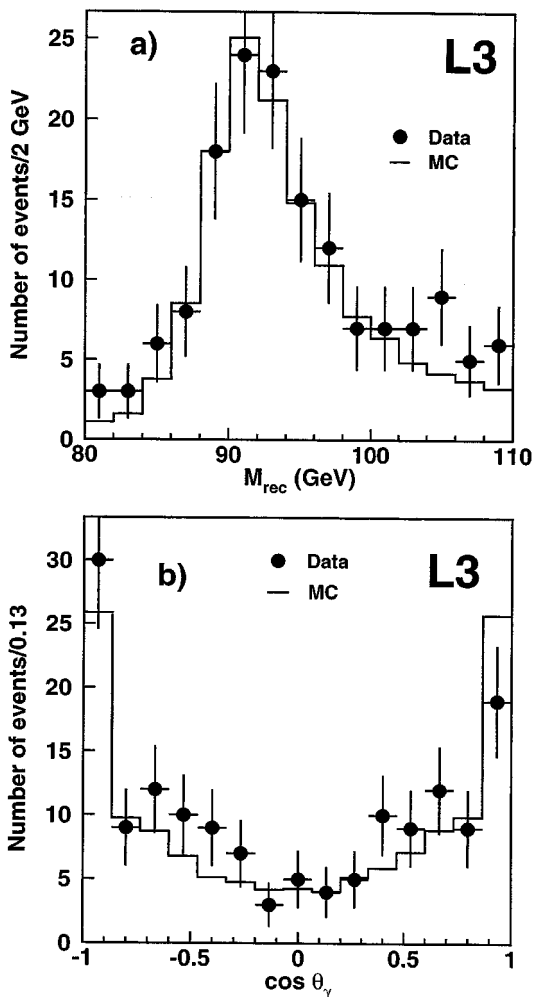
- The scintillator counters should provide signals in coincidence with the beam crossing time and should be associated to calorimetric clusters.

With these requirements 153 events are selected in the range from 161 GeV to 183 GeV. The acceptance of these cuts is estimated with the KORALZ Standard Model $e^+e^+ \to \nu\bar{\nu}\gamma(\gamma)$ generator [16]. The trigger efficiency is estimated to be above 99.7%.

All possible sources of background have been found to be negligible. Measured cross sections within the fiducial region defined in the previous section for the $q\bar{q}\gamma$ sample are shown in Table 2. They are in agreement with the expectations from the Standard Model. Fig. 3a and 3b show the distributions of the recoil mass and the polar angle of the photons, respectively. Good agreement between data and Standard Model Monte Carlo is observed.

3. Anomalous $ZZ\gamma$ and $Z\gamma\gamma$ couplings

The most general Lorentz invariant vertex functions in the presence of anomalous couplings are given in Ref. [22]. Deviations from the Standard Model are quantified in terms of eight anomalous couplings: h_i^V ($i = 1,4; V = \gamma,Z$), where a V superscript identifies a $ZV\gamma$ anomalous coupling. Compared to the Standard Model, all anomalous contributions to the cross section increase rapidly with the center-of-mass energy. In addition, h_1^V and h_2^V lead to CP-violating effects. In the Standard Model all eight couplings h_i^V are zero at tree level. At one loop level, only the CP conserving couplings h_3^V and h_4^V are nonzero and of order 10^{-4} [1,3].

An alternative choice of parameters is the following [12]:

$$\frac{\sqrt{\alpha}\, h_i^V}{m_Z^2} \equiv \frac{1}{\Lambda_{iV}^2}; \quad i = 1,3 \qquad (1)$$

$$\frac{\sqrt{\alpha}\, h_i^V}{m_Z^4} \equiv \frac{1}{\Lambda_{iV}^4}; \quad i = 2,4 \qquad (2)$$

In general, Lagrangians of dimension N lead to couplings $\Lambda^{-(N-4)}$. The couplings h_1^V and h_3^V receive contributions from operators of dimension 6, whereas h_2^V and h_4^V originate from operators of at

Fig. 3. Distributions of a) the mass recoiling against the photon $M_{\rm rec} = (s - 2E_\gamma\sqrt{s})^{1/2}$ and b) the polar angle of the photon in $e^+e^+ \to \nu\bar{\nu}\gamma(\gamma)$ events.

least dimension 8 [22]. Limits on h_i^V and Λ_{iV} are presented in the following subsections.

Due to unitarity constraints, the anomalous couplings h_i^V cannot get arbitrarily large values and should vanish in the limit $s \to \infty$ [23,2]. For experiments with variable s in the elementary collisions, a conventional choice for large values of the center-of-mass energy is to assume the following form-factor dependence [2,7–9]:

$$h_i^V = \frac{h_{i0}^V}{\left(1 + \dfrac{s}{\Lambda^2}\right)^3}; \quad i = 1,3 \tag{3}$$

$$h_i^V = \frac{h_{i0}^V}{\left(1 + \dfrac{s}{\Lambda^2}\right)^4}; \quad i = 2,4 \tag{4}$$

Form factors are not necessary in the case of e^+e^+ colliders under the assumption that the scale of new physics, Λ, is above the energy of the collision, $\sqrt{s}$. We will therefore assume $h_i^V \equiv h_{i0}^V$. In this way results are model independent and we also avoid hypotheses on the unknown behaviour when approaching energies close to the new physics scale Λ [24]. Limits on h_{i0}^V for the scale $\Lambda = 750$ GeV are determined below for comparison with other experiments.

3.1. Analysis procedure

A $e^+e^+ \to f\bar{f}\gamma$ event is described by the following five phase space variables: the photon energy E_γ, its polar and azimuthal angles θ_γ, ϕ_γ, and the angles of the fermion f in the center-of-mass frame of the Z system: θ_f^{CM}, ϕ_f^{CM}. The Z system is defined by a boost along the photon direction, with velocity:

$$v_Z = \frac{p_Z}{E_Z} = \frac{E_\gamma}{\sqrt{s} - E_\gamma} \tag{5}$$

We compute the Standard Model amplitude $\mathcal{M}_{SM}$ and the anomalous coupling amplitudes $\mathcal{M}_{AC}(h_i^V)$, ($i = 1,4$; $V = \gamma,Z$) of the process $e^+e^+ \to f\bar{f}\gamma$ following the formalism used in Ref. [22]. Effective Z couplings, non-resonant contributions like $e^+e^+ \to \gamma^*\gamma \to f\bar{f}\gamma$ and t-channel W-exchange corrections in $e^+e^+ \to \nu_e\bar{\nu}_e\gamma$ are also taken into account. Our calculations are in good agreement with those of Ref.

[2]. Distributions in the presence of anomalous couplings can be obtained from the corresponding Standard Model distributions at generator level by reweighting every event by the scale factor $w(E_\gamma, \theta_\gamma, \phi_\gamma, \theta_f^{CM}, \phi_f^{CM}; h_i^V)$:

$$w\left(E_\gamma, \theta_\gamma, \phi_\gamma, \theta_f^{CM}, \phi_f^{CM}; h_i^V\right)$$

$$= \frac{|\,(\mathcal{M}_{SM} + \mathcal{M}_{AC})\left(E_\gamma, \theta_\gamma, \phi_\gamma, \theta_f^{CM}, \phi_f^{CM}; h_i^V\right)|^2}{|\mathcal{M}_{SM}\left(E_\gamma, \theta_\gamma, \phi_\gamma, \theta_f^{CM}, \phi_f^{CM}\right)|^2} \tag{6}$$

Additional initial state radiation effects are taken into account by evaluating the expression at the center-of-mass of the $Z\gamma$ system. Monte Carlo studies show that the energy of additional photons is in most cases within the Z width and that changes in the event kinematics are not relevant.

The reweighting procedure is applied on reconstructed variables since the angular and energy detector resolutions do not modify significantly the ratio (6). For the $e^+e^+ \to \nu\bar{\nu}\gamma(\gamma)$ case, the neutrino angular variables need to be integrated out in both numerator and denominator. For the $e^+e^+ \to q\bar{q}\gamma(\gamma)$ process, the angles θ_f^{CM} and ϕ_f^{CM} are substituted by the angles of the thrust axis in the Z center-of-mass frame and the square of the amplitudes is symmetrized under the interchange $q \leftrightarrow \bar{q}$. The effect of this angle substitution is similar to the one studied in Ref. [25]. Compared to the present accuracy of the measurement, the possible bias on the final result is negligible.

Using the variables from the data sample allows the use of unbinned maximum-likelihood fits in the five-dimensional phase space. In order to quantify the possible contributions due to the anomalous couplings, we determine the value of a given anomalous coupling h_i^V that maximizes the following likelihood function:

$$\mathcal{L}\left(h_i^V\right) = \frac{N\left(h_i^V\right)_o^N \exp\left(-N\left(h_i^V\right)\right)}{N_o!}$$

$$\times \prod_{j=1}^{N_o} \frac{w_j\left(E_{\gamma j}, \theta_{\gamma j}, \phi_{\gamma j}, \theta_{f j}^{CM}, \phi_{f j}^{CM}; h_i^V\right)}{N\left(h_i^V\right)} \tag{7}$$

where, for each center-of-mass energy, N_o is the number of observed events and $N(h_i^V)$ is the number of expected events, determined by reweighting a large Monte Carlo sample. The expression $w_j / N(h_i^V)$ is proportional to the probability density of the event j.

The systematic effect due to the use of reconstructed energies and angles is estimated on the Monte Carlo sample by using reconstructed values instead of the generated ones. The uncertainty on E_γ changes the values of h_i^V by less than 0.02, due to the good L3 resolution and to the soft dependence of the weights w_j on E_γ. The bias due to the angular resolution for jets and photons is found to be an order of magnitude less significant.

4. Results

4.1. Limits on h_i^V

The data are found to be consistent with Standard Model expectations and hence with the absence of anomalous couplings. When studied independently, both $q\bar{q}\gamma$ and $\nu\bar{\nu}\gamma$ samples lead to the same conclusion. Most of the sensitivity to anomalous couplings comes from the $q\bar{q}\gamma$ channel alone, which has more statistics. The 95% confidence level (CL) limits on the parameters h_i^V from all $q\bar{q}\gamma$ and $\nu\bar{\nu}\gamma$ samples at center-of-mass energies between 161 GeV and 183 GeV are shown in Table 3.

Table 3

Limits on the anomalous $ZZ\gamma$ and $Z\gamma\gamma$ couplings obtained by combining the processes $e^+e^+ \to q\bar{q}\gamma(\gamma)$ and $e^+e^+ \to \nu\bar{\nu}\gamma(\gamma)$ at center-of-mass energies between 161 GeV and 183 GeV. The second column is obtained assuming form factors for a scale $\Lambda = 750$ GeV (Eqs. 3 and 4). In all fits, only one parameter is varied while the others are kept at zero.

95% CL Limits	95% CL Limits, $\Lambda = 750$ GeV
$-0.54 < h_1^Z < 0.17$	$-0.64 < h_{10}^Z < 0.20$
$-0.11 < h_2^Z < 0.37$	$-0.13 < h_{20}^Z < 0.47$
$-0.50 < h_3^Z < 0.36$	$-0.60 < h_{30}^Z < 0.42$
$-0.12 < h_4^Z < 0.39$	$-0.15 < h_{40}^Z < 0.50$
$-0.25 < h_1^\gamma < 0.23$	$-0.30 < h_{10}^\gamma < 0.28$
$-0.18 < h_2^\gamma < 0.18$	$-0.23 < h_{20}^\gamma < 0.23$
$-0.33 < h_3^\gamma < 0.01$	$-0.39 < h_{30}^\gamma < 0.06$
$-0.02 < h_4^\gamma < 0.24$	$-0.02 < h_{40}^\gamma < 0.30$

Table 4

Allowed regions at 95% CL for two-dimensional likelihood fits. In every fit all other six parameters are kept at zero.

Parameter	Fitted value	Lower limits	Upper limits	Correlation coefficient
h_1^Z	-0.24	-1.06	0.99	0.93
h_2^Z	0.02	-0.61	0.78	
h_3^Z	0.58	-0.68	1.25	0.81
h_4^Z	0.50	-0.34	0.97	
h_1^γ	-0.11	-0.72	0.63	0.96
h_2^γ	-0.09	-0.55	0.49	
h_3^γ	-0.26	-0.72	0.54	0.95
h_4^γ	-0.06	-0.45	0.48	
h_1^Z	-0.27	-0.60	0.28	-0.05
h_1^γ	0.03	-0.27	0.28	
h_2^Z	0.16	-0.17	0.42	-0.04
h_2^γ	-0.02	-0.21	0.20	
h_3^Z	-0.02	-0.50	0.46	-0.25
h_3^γ	-0.18	-0.36	0.08	
h_4^Z	0.13	-0.23	0.41	-0.30
h_4^γ	0.11	-0.07	0.26	
h_1^Z	-0.25	-0.60	0.28	-0.24
h_3^Z	-0.13	-0.55	0.43	
h_2^Z	0.14	-0.17	0.40	-0.21
h_4^Z	0.16	-0.21	0.43	
h_1^γ	-0.00	-0.27	0.25	0.04
h_3^γ	-0.18	-0.36	0.06	
h_2^γ	-0.00	-0.20	0.20	0.02
h_4^γ	0.12	-0.06	0.26	

The following sources of systematic errors are investigated:

- The bias due to the use of reconstructed angles and energies in the likelihood fit is estimated to be less than 0.02 (see Section 3 above), both for the $q\bar{q}\gamma$ and $\nu\bar{\nu}\gamma$ samples.
- Effects due to misidentification of the photon in $q\bar{q}\gamma$ events are studied on a large Monte Carlo sample of $Z \to q\bar{q}$ events. It is found to be 0.01.

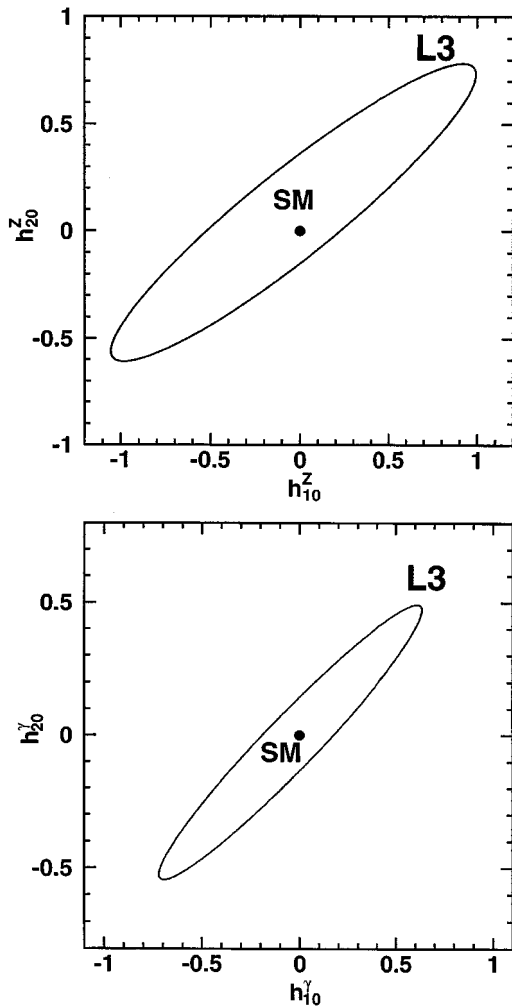Fig. 4. Contours at the 95% CL for the CP-violating coupling parameters, h_1^Z versus h_2^Z and h_1^γ versus h_2^γ. The Standard Model prediction is indicated by the dot.

- The contamination of $q\bar{q}e\nu$ events in $q\bar{q}\gamma$ events is studied by introducing a 1.5% background on the Monte Carlo signal. It changes the fit results by 0.02.
- An imperfect simulation of the detector could produce a bias in the analysis. The effect is estimated to be below 0.02 by comparing the differences introduced when the simulation is done neglecting all detector imperfections.

All these numbers are negligible compared to our present statistical sensitivity and do not affect the limits presented.

4.2. Two-dimensional fits

We have performed two-dimensional fits for several pairs of anomalous couplings, keeping the other six parameters fixed at zero. Allowed regions at the 95% CL are shown in Table 4. Within pairs of the same CP parity, (h_3^V, h_4^V) or (h_1^V, h_2^V), the correlations are found to be strong. The two-dimensional 95% limit contours for these pairs are shown in Fig. 4 and Fig. 5. We also show the limit obtained by D0 [9] for a value $\Lambda = 750\,\text{GeV}$.
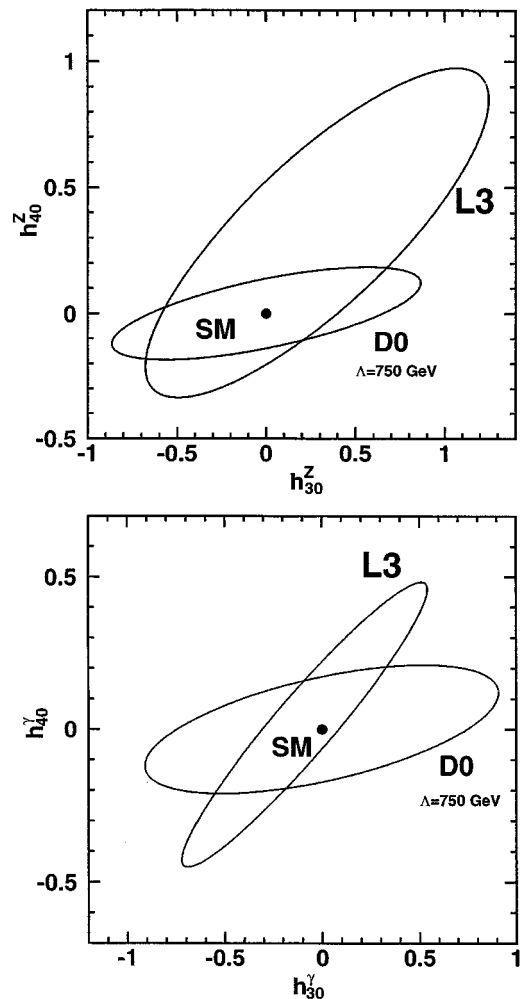

Fig. 5. Contours at the 95% CL for the CP-conserving coupling parameters, h_3^Z versus h_4^Z and h_3^γ versus h_4^γ. For comparison the results obtained by D0 assuming form factors with $\Lambda = 750\,\text{GeV}$ [9] are also shown. The Standard Model prediction is indicated by the dot.

Table 5
Limits on new physics scales producing anomalous $ZZ\gamma$ and $Z\gamma\gamma$ couplings. Fitted values and limits are obtained by combining the processes $e^+e^- \to q\bar{q}\gamma(\gamma)$ and $e^+e^- \to \nu\bar{\nu}\gamma(\gamma)$ at center-of-mass energies between 161 GeV and 183 GeV. In all fits, only one parameter is varied while the others are kept at zero.

Parameter	Fitted Value	Sensitivity
Λ_{1Z}	$\frac{1}{\Lambda_{1Z}^4} = (-0.27 \pm 0.17) \times 10^{-5}$	$\Lambda_{1Z} > 703\,\mathrm{GeV}$
Λ_{2Z}	$\frac{1}{\Lambda_{2Z}^6} = (+0.20 \pm 0.15) \times 10^{-9}$	$\Lambda_{2Z} > 218\,\mathrm{GeV}$
Λ_{3Z}	$\frac{1}{\Lambda_{3Z}^4} = (-0.18 \pm 0.21) \times 10^{-5}$	$\Lambda_{3Z} > 571\,\mathrm{GeV}$
Λ_{4Z}	$\frac{1}{\Lambda_{4Z}^6} = (+0.22 \pm 0.15) \times 10^{-9}$	$\Lambda_{4Z} > 213\,\mathrm{GeV}$
$\Lambda_{1\gamma}$	$\frac{1}{\Lambda_{1\gamma}^4} = (0.00 \pm 0.12) \times 10^{-5}$	$\Lambda_{1\gamma} > 636\,\mathrm{GeV}$
$\Lambda_{2\gamma}$	$\frac{1}{\Lambda_{2\gamma}^6} = (0.00 \pm 0.12) \times 10^{-9}$	$\Lambda_{2\gamma} > 255\,\mathrm{GeV}$
$\Lambda_{3\gamma}$	$\frac{1}{\Lambda_{3\gamma}^4} = (-0.19 \pm 0.09) \times 10^{-5}$	$\Lambda_{3\gamma} > 1082\,\mathrm{GeV}$
$\Lambda_{4\gamma}$	$\frac{1}{\Lambda_{4\gamma}^6} = (+0.15 \pm 0.08) \times 10^{-9}$	$\Lambda_{4\gamma} > 244\,\mathrm{GeV}$

Other two-dimensional fits show smaller correlations. This feature is confirmed by studies of Monte Carlo samples generated with non-zero CP-violating couplings. It indicates that CP-violating and CP-conserving effects, if present, can be disentangled.

4.3. Limits on new physics scales

We interpret our data in terms of physics scales using formulae (1) and (2), substituting the new parametrizations in the likelihood function (7). The results of the fit are shown in Table 5, together with the lower limits at the 95% CL on scales of new physics. To determine the confidence levels the probability distribution is normalized over the physically allowed range of the parameters ($\Lambda > 0$) [26].

5. Conclusions

We have performed a search for anomalous $ZZ\gamma$ and $Z\gamma\gamma$ couplings at LEP using the process $e^+e^- \to \nu\bar{\nu}\gamma(\gamma)$ and, for the first time, the process $e^+e^- \to q\bar{q}\gamma(\gamma)$. The analysis method exploits the full sensitivity of the differential cross section in both channels. Within this approach CP-violating effects are expected to be largely uncorrelated with CP-conserving ones and then, if present, distinguishable. No evidence for anomalous couplings is found. This result is quantified in a set of limits.

These limits are comparable in sensitivity to the limits obtained at the Tevatron [8,9]. Since there is no need of energy-dependent form factors at e^+e^- colliders, our limits are independent of the coupling behaviour at energies larger than $\sqrt{s}$. We exclude new physics scales below 213 GeV to 1083 GeV, depending on the type of anomalous coupling.

Acknowledgements

References

[1] F.M. Renard, Nucl. Phys. B 196 (1982) 93.
[2] U. Baur, E. Berger, Phys. Rev. D 47 (1993) 4889. The program for generating $f\bar{f}\gamma$ final states in the presence of anomalous $ZZ\gamma$ and $Z\gamma\gamma$ couplings was provided by Ulrich Baur.
[3] A. Barroso, F. Boudjema, J. Cole, N. Dombey, Z. Phys. C 28 (1985) 149.
[4] F.M. Renard, Phys. Lett. B 126 (1983) 59.
[5] M. Claudson, E. Farhi, R.L. Jaffe, Phys. Rev. D 34 (1986) 873.
[6] F. Boudjema, N. Dombey, Phys. Lett. B 351 (1995) 302.
[7] F. Abe et al., Phys. Rev. Lett. 74 (1995) 1941.
[8] S. Abachi et al., Phys. Rev. Lett. 78 (1997) 3640.
[9] B. Abbott et al., Phys. Rev. D 57 (1998) 3817.
[10] M. Acciarri et al., Phys. Lett. B 412 (1997) 201.
[11] P. Abreu et al., Phys. Lett. B 423 (1998) 194.
[12] P. Mery, M. Perrotet, F.M. Renard, Z. Phys. C 38 (1988) 579.
[13] D. Choudhury, S.D. Rindani, Phys. Lett. B 335 (1994) 198.
[14] L3 Collaboration, B. Adeva et al., Nucl. Instr. and Meth. A 289 (1990) 35; L3 Collaboration, M. Chemarin et al., Nucl. Instr. and Meth. A 349 (1994) 345; L3 Collaboration, M. Acciarri et al., Nucl. Instr. and Meth. A 351 (1994) 300; L3 Collaboration, A. Adam et al., Nucl. Instr. and Meth. A 383 (1996) 342.
[15] T. Sjöstrand, CERN–TH/7112/93 (1993), revised August 1995; T. Sjöstrand, Comput. Phys. Commun. 82 (1994) 74.

[16] S. Jadach, B.F.L. Ward, Z. Wąs, Comp. Phys. Comm. 79 (1994) 503.

[17] R. Kleiss, R. Pittau, Comp. Phys. Comm. 85 1995) 437.

[18] PHOJET version 1.10 is used. R. Engel, Z. Phys. C 66 (1995) 203; R. Engel, J. Ranft, Phys. Rev. D 54 (1996) 4244.

[19] J.H. Field, Phys. Lett. B 323 (1994) 432; J.H. Field, T. Riemann, Comput. Phys. Commun. 94 (1996) 53.

[20] D. Karlen, Nucl. Phys. B 289 (1987) 23.

[21] The L3 detector simulation is based on GEANT Version 3.15. R. Brun et al., GEANT 3, CERN–DD/EE/84–1 (Revised), 1987. The GHEISHA program (H. Fesefeldt, RWTH Aachen Report PITHA 85/02 (1985)) is used to simulate hadronic interactions.

[22] K. Hagiwara et al., Nucl. Phys. B 282 (1987) 253.

[23] H. Czyz, K. Kołodziej, M. Zrałek, Z. Phys. C 43 (1989) 97.

[24] J. Wudka, UCRHEP-T164 (1996).

[25] The LEP Heavy Flavour Group, *QCD corrections to $A_{FB}^{b\bar{b}}$ and $A_{FB}^{c\bar{c}}$ Measurements at LEP1*, LEPHF/97-01, ALEPH 97-081 PHYSIC 97-071, DELPHI 97-131 PHYS 720, L3 Note 2154, OPAL Technical Note TN500, 18 August 1997.

[26] R.M. Barnett et al., Review of Particle Properties Phys. Rev. D 54 (1996) 1 and references therein.